

Available online at www.sciencedirect.com

Chinese Journal of Aeronautics 21(2008) 411–416

**Chinese
Journal of
Aeronautics**www.elsevier.com/locate/cja

Numerical Computation of Stress Intensity Factors for Bolt-hole Corner Crack in Mechanical Joints

Wang Liqing*, Gai Bingzheng*Department of Astronautics and Mechanics, Harbin Institute of Technology, Harbin 150001, China*

Received 31 October 2007; accepted 2 February 2008

Abstract

The three-dimensional finite element method is used to solve the problem of the quarter-elliptical corner crack of the bolt-hole in mechanical joints being subjected to remote tension. The square-root stress singularity around the corner crack front is simulated using the collapsed 20-node quarter point singular elements. The contact interaction between the bolt and the hole boundary is considered in the finite element analysis. The stress intensity factors (SIFs) along the crack front are evaluated by using the displacement correlation technique. The effects of the amount of clearance between the hole and the bolt on the SIFs are investigated. The numerical results indicate that the SIF for mode I decrease with the decreases in clearance, and in the cases of clearance being present, the corner crack is in a mix-mode, even if mode I loading is dominant.

Keywords: bolt-hole corner crack; contact; stress intensity factor; mechanical joint; clearance; finite element method

1 Introduction

As a joining technique, mechanical joints such as bolted or riveted joints are widely used in aerospace structures. Cracks often exist at the hole-edge because of stress concentration, contact interaction between the hole and the bolt, or the manufacturing process. It is necessary to determine stress intensity factors (SIFs) in order to evaluate the crack growth, residual strength, and fatigue life of the cracked structures.

Many researchers have investigated the SIFs for the cracks at the hole-edge. However, there are only a few studies that take into consideration contact interaction between the hole and the bolt or the contact pressure that develops in the hole boundary^[1–5]. The effects of the changes in clearance be-

tween the bolt and the hole on SIFs along the crack front, for a bolt-hole corner crack, appear to be absent in relevant literatures. In fact, a corner crack typically occurs at the surface of a component and it can be simulated as a quarter-elliptical shape^[6]. The part-through nature of the corner crack necessitates three dimensional analysis to determine the SIFs. The problem of the bolt-hole corner crack is quite complicated when the contact interaction between the hole and bolt is considered. In general, the contact region and contact pressure depend on the external load and the elasticity properties of the material being used. Such dependence converts the contact problem into being nonlinear and as such the only possible way to solve this problem is to use numerical methods such as the finite element method (FEM) and boundary element method^[7].

In this article, the mix-mode SIFs along the crack front for mechanical joints with a bolt-hole corner crack, under remote tensions, are analyzed

*Corresponding author. Tel.: +86-451-55693608.

E-mail address: wangliq1965@163.com

Foundation item: National Natural Science Foundation of China (10272036)

using the general purpose finite element analysis software ANSYS, and the effects of the amount of clearance between the hole and the bolt on the SIFs along the crack front are investigated.

2 Computational Method of SIFs

In the fracture analysis, in order to simulate the square-root stress singularity around the corner crack front, the collapsed 20-node quarter point singular elements are usually utilized. These elements are depicted in Fig.1.

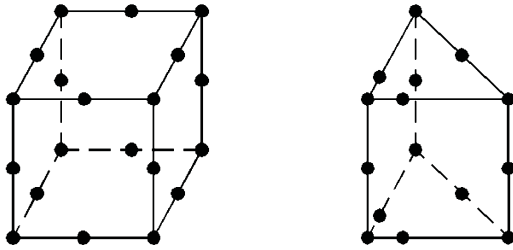


Fig.1 Brick elements and quarter-node singular elements.

Assuming that there is a quarter-elliptical corner crack of length c and depth a at the bolt-hole in the mechanical joints, as shown in Fig.2. A point, P , at the crack front, can be positioned by the parametric angle α and accordingly the crack-tip local coordinate system (t, n, s) at point P can also be positioned, where t , n , and s are in tangential, normal, and binormal directions, respectively.

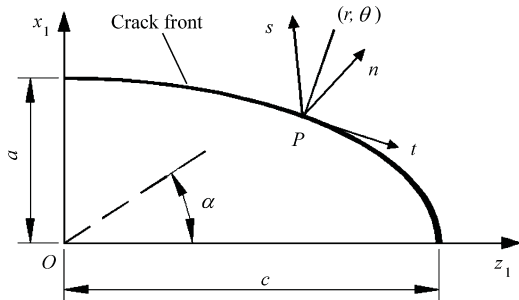


Fig.2 Quarter-elliptical corner crack and the crack-tip local coordinate system at point P .

The displacement correlation technique (DCT) can be used to calculate the SIFs. Note that the asymptotic expressions for the three dimensional problem and plane strain problem are identical except at the point where the crack front intersects a

traction free boundary^[8]. Hence, the asymptotic distribution of the displacement components in the vicinity of point P can be expressed as^[9]

$$u_s(r, \theta) = \frac{K_I}{4\mu} \sqrt{\frac{r}{2\pi}} \left[(2\kappa + 1) \sin \frac{\theta}{2} - \sin \frac{3\theta}{2} \right] - \frac{K_{II}}{4\mu} \sqrt{\frac{r}{2\pi}} \left[(2\kappa - 3) \cos \frac{\theta}{2} + \cos \frac{3\theta}{2} \right] \quad (1)$$

$$u_n(r, \theta) = \frac{K_I}{4\mu} \sqrt{\frac{r}{2\pi}} \left[(2\kappa - 1) \cos \frac{\theta}{2} - \cos \frac{3\theta}{2} \right] + \frac{K_{II}}{4\mu} \sqrt{\frac{r}{2\pi}} \left[(2\kappa + 3) \sin \frac{\theta}{2} + \sin \frac{3\theta}{2} \right] \quad (2)$$

$$u_t(r, \theta) = 2 \frac{K_{III}}{\mu} \sqrt{\frac{r}{2\pi}} \sin \frac{\theta}{2} \quad (3)$$

where K_I , K_{II} , and K_{III} denote the SIFs for modes I, II, and III, respectively; μ is the shear modulus; κ is equal to $3 - 4\nu$, ν is the Poisson ratio; and r and θ are position coordinates (see Fig.2).

Evaluating Eqs.(1)-(2) for $\theta = \pm\pi$, the SIF for mode I can be expressed as

$$K_I = \lim_{r \rightarrow 0} \sqrt{2\pi} \frac{\mu}{\kappa + 1} \frac{\Delta u_s}{\sqrt{r}} \quad (4)$$

where Δu_s is the relative displacement component of one crack surface with respect to the other in the s direction at position r .

It can be found from Eq.(4) that K_I depends on the $\Delta u_s / \sqrt{r}$ value at position $r \rightarrow 0$. In order to calculate the SIF for mode I, the authors first take a section at point P parallel to the normal plane (n, s) . The section and the deformed shape of the crack are shown in Fig.3, where R_1 and R_2 are the distances of

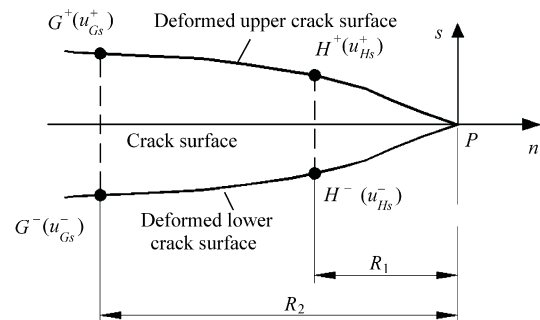


Fig.3 Deformed shape of the crack surfaces.

point P to the point H^+ (or H^-) and point G^+ (or G^-) of undeformed configuration, respectively.

Points H^+ , G^+ , H^- , and G^- should be located on the edge of the selected quarter-node singular elements of the upper and lower crack surfaces, respectively. The displacement components of these points, u_{Hs}^+ , u_{Gs}^+ , u_{Hs}^- , and u_{Gs}^- , can be obtained by the path operations of ANSYS. Thus, the relative displacements in the s direction on the locations of $r = R_1$ and $r = R_2$ can be expressed as

$$\Delta u_{Hs} = u_{Hs}^+ - u_{Hs}^- \quad (5)$$

$$\Delta u_{Gs} = u_{Gs}^+ - u_{Gs}^- \quad (6)$$

With the displacement extrapolation method^[10], the values of $\Delta u_s / \sqrt{r}$ taken from the finite element results can be written as

$$\frac{\Delta u_{Hs}}{\sqrt{R_1}} = A_1 + A_2 R_1 \quad (7)$$

$$\frac{\Delta u_{Gs}}{\sqrt{R_2}} = A_1 + A_2 R_2 \quad (8)$$

where A_1 and A_2 are constants.

Using Eqs.(7)-(8), and Eq.(4), and letting r approach 0, the SIF for mode I can be evaluated by

$$K_I = \sqrt{2\pi} \frac{\mu}{\kappa + 1} \left[\frac{\Delta u_{Hs} R_2^{3/2} - \Delta u_{Gs} R_1^{3/2}}{\sqrt{R_1 R_2} (R_2 - R_1)} \right] \quad (9)$$

Similarly, the SIFs for modes II and III can also be obtained

$$K_{II} = \sqrt{2\pi} \frac{\mu}{\kappa + 1} \left[\frac{\Delta u_{Hn} R_2^{3/2} - \Delta u_{Gn} R_1^{3/2}}{\sqrt{R_1 R_2} (R_2 - R_1)} \right] \quad (10)$$

$$K_{III} = \sqrt{2\pi} \frac{\mu}{4} \left[\frac{\Delta u_{Ht} R_2^{3/2} - \Delta u_{Gt} R_1^{3/2}}{\sqrt{R_1 R_2} (R_2 - R_1)} \right] \quad (11)$$

where Δu_{Hn} , Δu_{Gn} , Δu_{Ht} , and Δu_{Gt} are the relative displacements in the n and t directions, on the locations of $r = R_1$ and $r = R_2$, respectively.

Once the displacement field of the cracked structure is computed using ANSYS, the SIFs for three fracture modes can be determined by DCT.

3 Model Validation and Comparison

To validate the finite element analysis tech-

nique used in the present study, the authors provide some comparisons of the results given by Walters, et al.^[11]. The geometry and loading of the cracked plate problem considered by Walters, et al. are depicted in Fig.4.

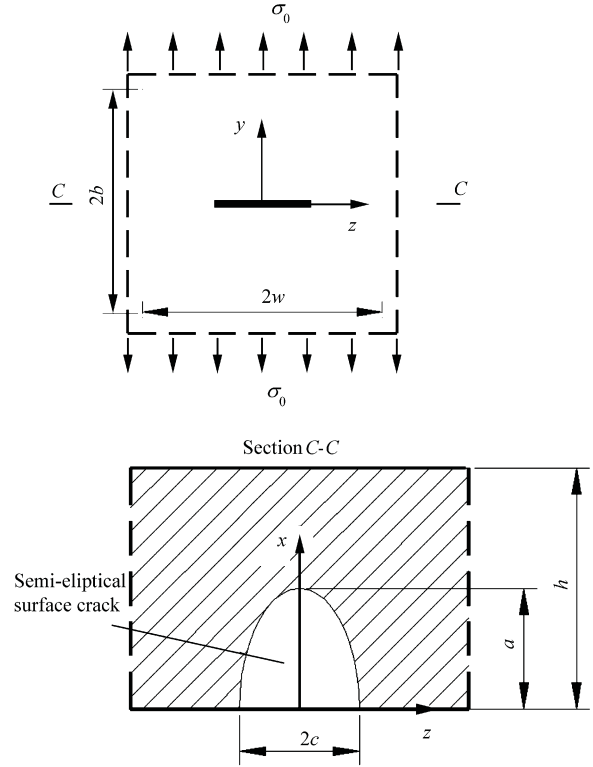


Fig.4 Geometry and loading of the surface cracked plate.

The dimensions of $2b$ and $2w$ should be taken as being sufficiently large to enable the calculated SIFs to approximate those calculated for a semi-infinite plate. Here, the specimen dimensions are taken as $2b = 2w = 1.2$ m, $h = 0.1$ m, and $a = h/2$, and the crack aspect ratio is $a/c = 2$. The material properties are elastic modulus $E = 10$ GPa and the Poisson ratio $\nu = 0.25$. Only a quarter of the cracked plate is analyzed because of symmetry.

The comparison of the normalized SIF for mode I are shown in Fig.5. The normalized SIF for mode I is defined as

$$K_I^n = K_I / (\sigma_0 \sqrt{\pi a / Q}) \quad (12)$$

$$Q = 1 + 1.464(c/a)^{1.65} \quad (13)$$

It can be found from Fig.5 that the calculated results of the present study are in good agreement with those given by Walters, et al.

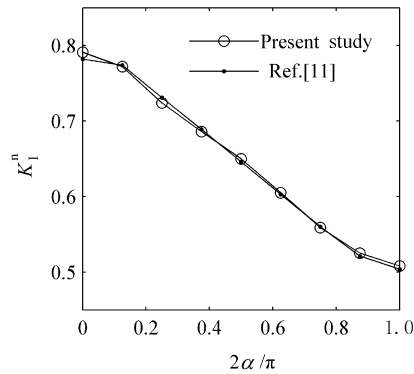
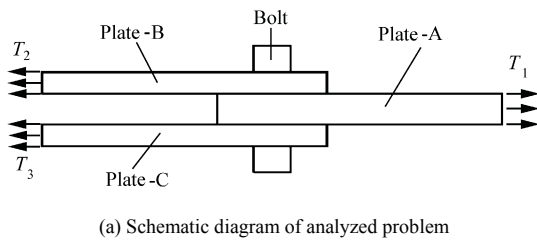


Fig.5 Comparison of the normalized SIF for mode I.

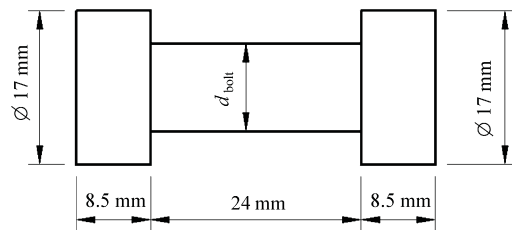
4 Numerical Computation of SIFs for Bolt-hole Corner Crack

4.1 Problem description

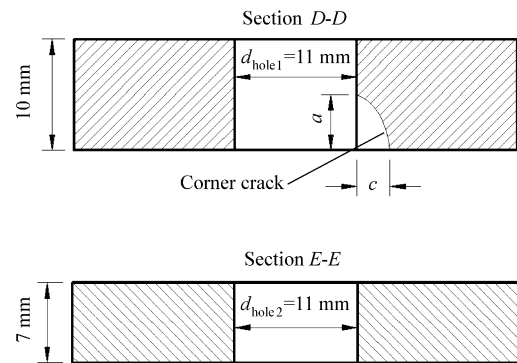
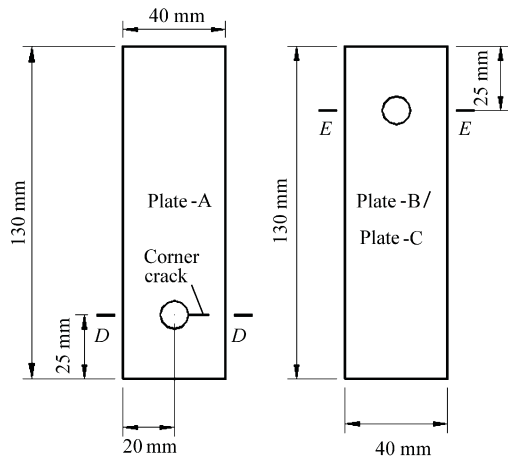
The geometries and loadings of the cracked mechanical joints are depicted in Fig.6, where T_1 and $T_2 = T_3$ are the applied uniform remote tensions,



(a) Schematic diagram of analyzed problem



(b) Detail of bolt



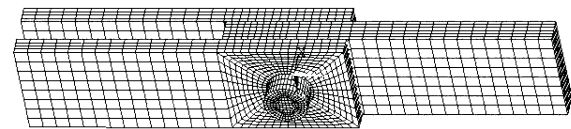
(c) Details of plate-A, plate-B, and plate-C

Fig.6 Geometries and loadings of the cracked structure.

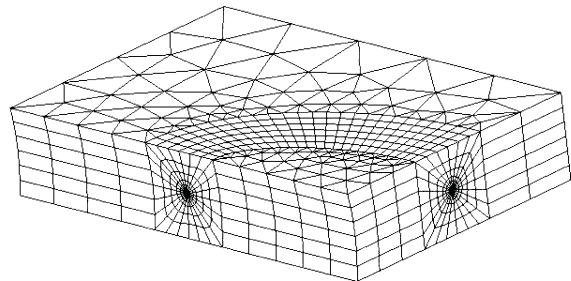
and d_{hole1} , d_{hole2} , and d_{bolt} are the diameters of the holes and pin, respectively. A single quarter-elliptical corner crack of length c and depth a is located on the bolt-hole of plate-A. The dimensions for the bolt-hole corner crack are $c = 3$ mm and $a = 5$ mm. The material properties are elastic modulus $E = 210$ GPa and Poisson ratio $\nu = 0.3$.

4.2 Finite element model

To obtain convergent results, the mesh density, number, and size of the quarter point singular elements around the crack front have to be considered carefully. The finite element model used in the present study is depicted in Fig.7.



(a) Whole mesh



(b) Close-up view of the elements around the crack front

Fig.7 Finite element model.

There are a total of 18 116 three dimensional brick elements in the model. About 600 of these elements are the singular elements that are used

around the crack front. The ratio of the radius of quarter point singular element to the crack depth a is taken as 0.02. The contact areas between the holes and the bolt are modeled by 2 118 surface to surface contact elements. The total number of nodes of the model is 36 639, hence the total number of degrees of freedom is $36\ 639 \times 3$. Only the case of frictionless contact is considered in the present study.

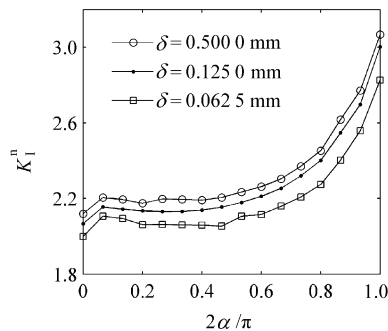
4.3 Results and discussions

The model mentioned earlier in this article is solved using ANSYS FEM code and the SIFs for mix-mode are calculated by Eqs.(9)-(11). To examine the effects of the amount of clearance between the hole and the bolt on the SIFs, the clearances, $\delta = (d_{\text{hole}} - d_{\text{bolt}})/2$, are set to 0.500 0, 0.125 0, 0.062 5 mm, respectively. The calculated SIFs of these three simulations are normalized into nondimensional ones according to

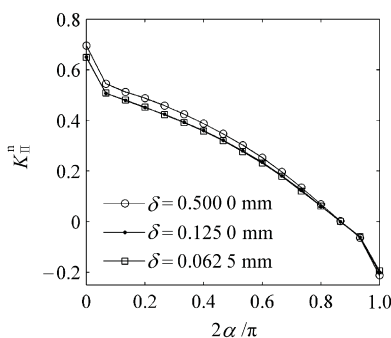
$$K_M^n = K_M / (T_1 \sqrt{\pi a / Q}) \quad (14)$$

where $M = \text{I, II, and III}$, and the normalization factor Q is given by Eq.(13).

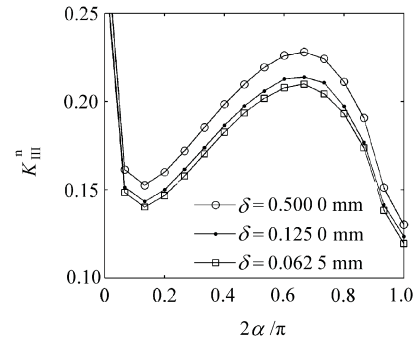
Fig.8 depicts the normalized SIFs around the crack front for three different clearances.



(a) Mode I



(b) Mode II



(c) Mode III

Fig.8 Effects of the amount of clearance on SIFs for a quarter-elliptical corner crack on the bolt-hole.

In Fig.8, $2\alpha/\pi=0$ corresponds to the c -tip, and $2\alpha/\pi=1$ to the a -tip.

It can be seen from Fig.8(a) that the SIF for mode I along the crack front decreases with a decrease in the clearance between the hole and the bolt. These results indicate that the amount of clearance has a significant influence on the SIF for mode I, and its proper consideration is required to evaluate the crack growth, residual strength, and fatigue life of the cracked mechanical joints. It can also be seen from Fig.8(a) that the SIF for mode I reaches a maximum value when the parametric angle $\alpha=\pi/2$.

It can be found from Figs.8(b)-8(c) that the SIFs for mode II and mode III along the crack front are smaller than that for mode I, but their values cannot be neglected. This demonstrates that in the case of the existing clearance, a quarter-elliptical corner crack on the bolt-hole of mechanical joints cannot be considered as pure mode I even if the loading of mode I is dominant.

It can be observed from Fig.8 that the SIFs based on plane strain conditions and square-root singularity definition, exhibit phenomena of sharp changes at the intersection ($2\alpha/\pi=0$) of the crack front with the free surface of plate-A. It is a well-known result for linear elastic fracture mechanics that the stress near the crack tip exhibits a singularity of $r^{-0.5}$, where r is the distance measured from the crack tip. However, it has been proved by Ben-them^[12-13] that this classical singularity does not hold at the intersection of the three-dimensional crack front with the free surface, but instead a singularity of the form r^λ exists. The singularity ex-

ponent λ is found to be a function of the fracture modes (i.e., modes I, II or III), the inclination angle β of the crack front relating to the free surface, the angle γ between the crack plane and the solid surface, and the Poisson ratio of the material used. As a result, the calculated SIFs of the present study, similar to many numerical solutions, exhibit sharp changes at the intersection, ($2\alpha/\pi=0$), of the crack front with the free surface because of the complex nature of the stress singularity of that point. Researches have shown that the zone with nonsquare-root singularity comprises of only a very small fraction of the crack edge^[14-15]. Therefore, the change of stress singularity can be neglected from the application's point of view.

5 Conclusions

The three-dimensional FEM and DCT are used to determine the SIFs of mechanical joints with quarter-elliptical corner crack on the bolt-hole. The following conclusions can be drawn:

(1) The SIF for mode I reaches its maximum value when the parametric angle is $\alpha=\pi/2$.

(2) The SIF for mode I along the crack front decrease with a decrease in clearance between the hole and the bolt. These results indicate that the amount of clearance has a significant influence on the SIF for mode I.

(3) In the case of the existing clearance, quarter-elliptical corner cracks on the bolt-holes of mechanical joints are in a mix-mode even if the loading of mode I is dominant.

References

- [1] Ju S H. Stress intensity factors for cracks in bolted joints. *International Journal of Fracture* 1997; 84(2): 129-141.
- [2] Cartwright D J, Parker A P. Opening mode stress intensity factors for cracks in pin-loads joints. *International Journal of Fracture* 1982; 18(1): 65-78.
- [3] Ju S H, Horng T L. Behaviors of a single crack in multiple bolted joints. *International Journal of Solids and Structures* 1999; 36(27): 4055-4070.
- [4] Chiang Y J, Rowlands R E. Finite elements analysis of mix-mode of fracture of bolted composite joints. *Journal of Composites Technology and Research* 1991; 13(4): 227-235.
- [5] Heo S P, Yang W H. Stress intensity factor analysis of elliptical corner cracks in mechanical joints by weight function method. *International Journal of Fracture* 2002; 115(4): 377-399.
- [6] Heo S P, Yang W H. Approximate weight function method for elliptical arc through cracks in mechanical joints. *Engineering Fracture Mechanics* 2003; 70(9): 1171-1192.
- [7] Wen P H, Aliabadi M H. Approximate dynamic crack frictional contact analysis for 3D structure. *Journal of the Chinese Institute of Engineers* 1999; 22(6): 785-793.
- [8] Yildirim B, Dag S, Erdogan F. Three dimensional fracture analysis of FGM coating under thermomechanical loading. *International Journal of Fracture* 2005; 132(4): 369-395.
- [9] Fan T Y. Theoretical foundation of fracture. Beijing: Science Press, 2003; 113-188. [in Chinese]
- [10] Banks-Sills L. Application of the finite element method to linear elastic fracture mechanics. *Applied Mechanics Reviews* 1991; 44(10): 447-461.
- [11] Walters M C, Paulino G H, Dodds R H. Stress-intensity factors for surface cracks in functionally graded materials under mode-I thermomechanical loading. *International Journal of Solids and Structures* 2004; 41(3-4): 1081-1118.
- [12] Benthem J P. State of stress at the vertex of a quarter-infinite crack in a half-space. *International Journal of Solids and Structures* 1977; 13(5): 479-492.
- [13] Benthem J P. The quarter-infinite crack in a half-space: alternative and additional solutions. *International Journal of Solids and Structures* 1980; 16(2): 119-130.
- [14] Ayhan A O, Nied H F. Stress intensity factors for three dimensional surface cracks using enriched finite elements. *International Journal for Numerical Methods in Engineering* 2002; 54(6): 899-921.
- [15] He M Y, Hutchinson J W. Surface crack subject to mixed mode loading. *Engineering Fracture Mechanics* 2000; 65(1): 1-14.

Biographies:

Wang Liqing Born in 1965, he is a Ph.D. candidate in Harbin Institute of Technology. His main research interests include analytical, numerical, and experimental aspects of structural strength.

E-mail: wanglq1965@163.com

Gai Bingzheng Born in 1941, he is a professor and doctoral supervisor in Harbin Institute of Technology. His main research interest involves solid dynamics.

E-mail: gaibz@hit.edu.cn